Volume-Translated Equations of State: Empirical Approach and Physical Relevance

Leonid V. Yelash and Thomas Kraska
Institute of Physical Chemistry, University of Cologne, D-50939 Köln, Germany

The volume translation technique is widely applied in chemical engineering modeling of phase behavior and thermodynamic properties. This empirical correction of the molar volume improves the correlation of liquid densities when cubic equations of state are employed. Based on a recently proposed method of analyzing equations of state, the influence of the volume translation on the properties obtained from an equation of state, such as virial coefficients, as well as on the phase behavior, critical properties, the isobaric thermal expansion coefficient, and the heat capacities of pure substances is investigated. The influence of different kinds of temperature-dependent volume translations is investigated and compared to approaches that originate from theoretical considerations. The investigation shows that empirical as well as theoretical approaches for the development of equations of state can exhibit nonphysical behavior. However, the understanding of the reasons for such problems can help to develop reliable equations of state based on both kinds of method.

Introduction

Cubic equations of state, which usually originate from the van der Waals equation of state, are most widely employed in chemical engineering applications. A shortcoming of the van der Waals-like cubic equations of state is the accuracy of the calculated saturated-liquid volumes. The derivation of the van der Waals (vdW) repulsion term includes several crude approximations. As a result, several properties calculated with the vdW equation of state deviate from the corresponding theoretical values. For example, the vdW repulsion term diverges to infinite pressure at the packing fraction $y = 0.25$. This is approximately one-third of the maximal possible packing fraction of spheres, which is $y = 0.7406$. A way to address this problem is to use the Carnahan−Starling (CS) repulsion term (Carnahan and Starling, 1969), which has been derived by summation of the virial series for the hard-sphere fluid. The CS repulsion diverges at a packing fraction, $y = 1$, which is one-third above the theoretical value. Nevertheless, the CS equation accurately reproduces the properties of the hard-sphere fluid, which is often employed to model repulsion forces. Replacing the vdW repulsion by the CS repulsion has the disadvantage that the mathematical structure of the equation of state becomes more complicated, that is, it cannot be kept cubic. Since cubic equations of state are employed in many industrial applications, other approaches to improve the modeling of the saturated liquid volumes have been developed. One of these methods is the volume translation technique (Martin, 1979; Peneloux et al., 1982; Chou and Prausnitz, 1989; Ji and Lempe, 1997; Ahlers and Gmehling, 2001). In the simplest case, the volume in an equation of state is replaced by a new volume shifted by a constant value.

Here we investigate the volume translation with respect to theoretical features of the resulting equation of state based on the method proposed recently for general repulsion and attraction terms (Yelash and Kraska, 1999a, 2001; Yelash, 2002). This work is about qualitative behavior and general equation-of-state structures. Therefore, throughout this work reduced variables are used. The way of reducing the variables and the connection to real units is given whenever they are used.

Equation of State

We consider the vdW equation of state as an example of a

Correspondence concerning this article should be addressed to T. Kraska.

cubic equation of state

$$p = \frac{RT}{V - b} - \frac{a}{V^2} \tag{1}$$

Using this simplest possible equation of state helps avoiding possible artifacts that may be caused by a mathematically complicated structure. The vdW equation is usually not considered for quantitative correlations; however, the results obtained in this investigation can be applied to more quantitative equations of state as well.

The volume translation can be introduced by replacing the volume V by $V + c$

$$p = \frac{RT}{V + c - b} - \frac{a}{(V + c)^2} \tag{2}$$

In order to analyze the influence of the volume translation on the properties of an equation of state, we rearrange Eq. 1 by introducing the packing fraction $y = b/4V$. Furthermore, a dimensionless volume translation parameter $f = c/b$, similar to that suggested in the literature (Jhaveri and Youngren, 1988), is introduced. The resulting pressure equation is given by Eq. 3, and the compressibility factor is given by Eq. 4

$$p = RT\frac{4y}{b}\left(\frac{1}{1-(4-4f)y}\right) - \frac{16a}{b^2}y^2\left(\frac{1}{(1+4fy)^2}\right) \tag{3}$$

$$Z = \frac{pV}{RT} = \left(\frac{1}{1-(4-4f)y}\right) - \frac{1}{T^*}\left(\frac{y}{(1+4fy)^2}\right) \tag{4}$$

Here T^* is the reduced temperature defined by $T^* = RTb/4a$. Furthermore, the virial coefficients of the repulsion and the attraction terms are calculated for the analysis of the volume-translated vdW equation

$$Z = Z_{\text{rep}} + Z_{\text{att}} \tag{5}$$

with

$$Z_{\text{rep}} = 1 + \sum_{i=1}^{\infty} (4 - 4f)^i y^i \tag{6}$$

$$Z_{\text{att}} = \frac{1}{T^*}\sum_{i=1}^{\infty} -i(-4f)^{i-1} y^i \tag{7}$$

From the latter two equations one can obtain the expressions for the repulsive and the attractive virial coefficients

$$B_{i+1,\text{rep}} = (4 - 4f)^i \tag{8}$$

$$B_{i+1,\text{att}} = -\frac{1}{T^*} i(-4f)^{i-1} \tag{9}$$

It is of interest to note that the volume translation affects the second virial coefficient of the repulsion term but not the second virial coefficient of the attraction term. Furthermore, one can see that the volume translation introduces the attractive virial coefficients beyond $B_{2,\text{att}}$ which are zero for the original vdW attraction. For the Redlich–Kwong (RK) (Redlich and Kwong, 1949) attraction or the Peng–Robinson (PR) (Peng and Robinson, 1976) attraction, the virial coefficients beyond $B_{2,\text{att}}$ are already nonzero and the volume translation only changes them.

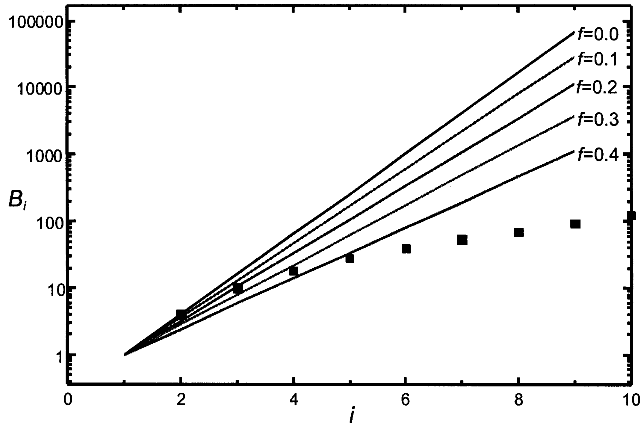

Figure 1. Logarithmic plot of the repulsive virial coefficients against the index of the virial coefficient.

The symbols are theoretical values taken from the literature (Ree and Hoover, 1964, 1967; Janse van Rensburg, 1993). The lines represent the values calculated for different values of the volume translation parameter, f, as indicated in the figure.

The repulsive virial coefficients can be analyzed in a recently proposed way in the ln $B_{\text{i,rep}}(i)$ diagram (Yelash and Kraska, 2001; Yelash, 2002) shown in Figure 1. In this diagram the vdW virial coefficients appear as a straight line with positive slope. Figure 1 shows the virial coefficients of the vdW equation of state with different values of the volume translation parameter up to $f = 0.4$. One can see that all virial coefficients are represented by straight lines with different slopes. The fix point for all lines is the ideal gas limit at $i = 1$ (ln $B_{i,\text{rep}} = 0$). Increasing volume translation shifts the virial coefficients toward the theoretical values. The curvature of ln $(B_{i,\text{rep}})$ as a function of i, of course, cannot be represented by a linear function. As shown recently (Yelash and Kraska, 2001; Yelash, 2002), the slope of these lines is related to the maximal packing fraction of the repulsion term at which the pressure diverges. This so-called pole-packing fraction y_{pole} is given here by

$$y_{\text{pole}} = \frac{1}{4 - 4f} \tag{10}$$

The dependence of the pole-packing fraction on the volume-translation parameter, f, is shown in Figure 2. One can see that for the vdW equation with $f = 0$ the pole-packing fraction is 0.25. As the volume translation parameter increases, the pole-packing fraction increases. It is shown up to $y_{\text{pole}} = 1.0$, which corresponds to $f = 0.75$. Further increase of f toward 1.0 yields a diverging pole-packing fraction. The upper limit of f corresponding to $y_{\text{pole}} = 0.75$, which is roughly

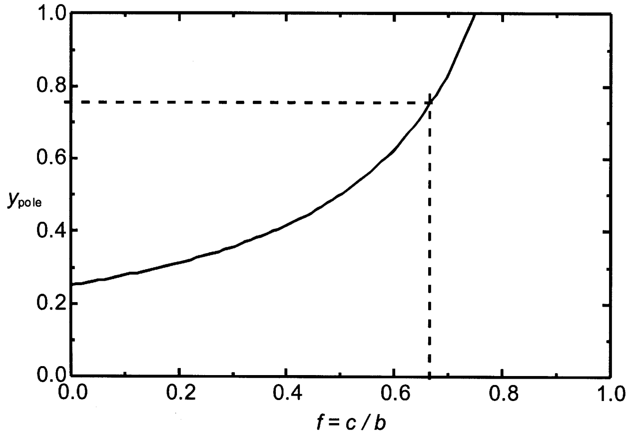

Figure 2. Calculated pole-packing fraction as a function of the volume-translation parameter, f, calculated from Eq. 3.

The dashed lines indicate the value of f corresponding to the physical limit of the packing fraction close to $y = 0.75$.

the close packing of hard spheres, can be estimated from Figure 2 at about $f = 0.66$.

In conclusion, a constant volume shift improves the values of the higher repulsion virial coefficients and the value of the pole-packing fraction. On the other hand, it lowers the second virial coefficient, which is exact for the hard-sphere fluid in the original vdW repulsion. Furthermore, it does not affect the curvature of the $\ln(B_{i,\mathrm{rep}})$ plot, which is not zero for the lower virial coefficients in contrast to the vdW repulsion.

Critical Properties and Phase Equilibria

In this section the effect of the volume translation on the phase equilibria and critical properties is investigated. The critical compressibility factor depends on the volume-translation parameter f. This dependence is linear if the vdW equation is used as reference equation ($Z_c = -1/8f + 3/8$). As shown recently (Yelash and Kraska, 1999a), the decrease in the critical compressibility factor is related to alternating signs of the attractive virial coefficients (Eq. 9). For the physical limit at $f = 0.66$, one can reach a critical compressibility factor of about 0.3. The corresponding dependence of the critical packing fraction is given by $1/y_c = -4f + 12$. It follows that the critical molar volume is linear dependent on the volume-translation parameter, f.

The volume translation has no influence on the reduced critical temperature and pressure; it rather selectively affects the critical packing fraction and volume. As a result, the vapor-pressure curve does not change for different values of the volume-translation parameter, f; it remains exactly the same as for the vdW reference equation. The effects of the volume translation on the coexistence curves in the temperature–density diagram and in the pressure–density diagram are shown in Figure 3. In these diagrams all properties are reduced to the corresponding critical values in order to make the results comparable. Figure 3 shows that at different temperatures different volume-translation parameters reproduce the liquid density well. With increasing temperature, the values of f that reproduce the experimental data also increase. This may suggest that a temperature-dependent volume translation parameter can be introduced. However, it has been shown that a temperature-dependent volume translation can lead to an unphysical crossing of the isotherms (Pfohl, 1999). We revisit this problem later in this article.

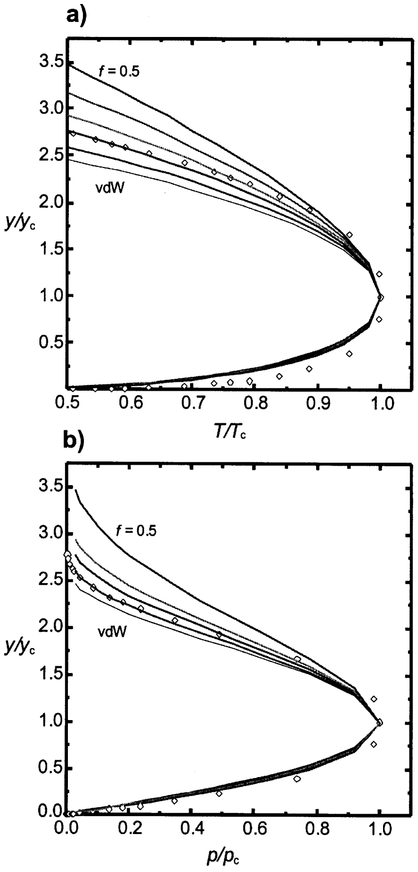

Figure 3. Coexistence curves calculated with Eq. 3 for different volume translation parameters f.

(a) packing-fraction-temperature plot; (b) packing-fraction-pressure plot. All data are reduced by the critical values. The symbols are experimental data for the coexistence curve of methane (Vargaftik, 1975).

Volume Translation in a Master Diagram

In order to analyze the effect of the volume translation more systematically, we have plotted in Figure 4 the effect of the volume translation on the master diagram, as suggested recently (Yelash and Kraska, 1999a) for a general attraction term. The axes of this diagram are the coefficients k and m of the general density dependence of the attraction term

$$p_{\mathrm{att}} = -\frac{a}{(V + mb)(V + kb)} \qquad (11)$$

This equation is a Peng–Robinson-like attraction term generalized by the parameters k and m. A specific equation of state has a certain set of parameters (k,m). For example, for

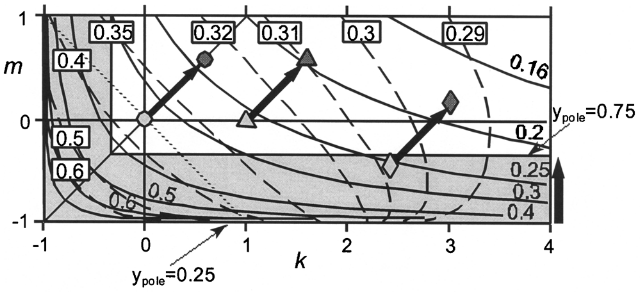

Figure 4. Master diagram for a generalized Peng–Robinson attraction term (Eq. 11).

Circle: van der Waals; triangle: Redlich–Kwong; diamond: Peng–Robinson. The corresponding symbols at the arrowheads are the same equations for $f = 0.66$. Dashed curves: constant Z_c, as given in the boxes; solid curves: constant y_c/y_{pole}, as indicated at the curves. All curves are calculated for $f = 0$ and represent roughly the trend of the volume translation. The symbols arrowtails correspond to the limit $y_{\text{pole}} = 0.25$, the symbols at the arrowheads correspond to the limit at $y_{\text{pole}} = 0.75$.

the vdW equation this set is (0,0), for the Redlich–Kwong equation it is (1,0), and for the Peng–Robinson equation it is $(1+\sqrt{2}, 1-\sqrt{2})$. The volume translation increases the values of m and k, and, hence, changes the position of these equations in the master diagram along the bold arrows in Figure 4. The arrowheads are at $f = 0.66$, which corresponds to the physical limit $y_{\text{pole}} = 0.75$. In the master diagram, curves at constant critical compressibility factor (dashed lines, numbers in boxes) also are shown. The volume translation also affects the repulsion term, and, hence, the accessible area of the master diagram that is limited by the pole-packing fraction at low values of m and k. The limits $y_{\text{pole}} = 0.25$ and $y_{\text{pole}} = 0.75$ are marked in Figure 4.

Correction of the Second Virial Coefficient

The introduction of the volume translation has an effect on the virial coefficients of the repulsion term, as shown in Figure 1. In general the virial coefficients are closer to the theoretical values if f increases. However, there is no unique value of f that reproduces all virial coefficients correctly. Actually, the second virial coefficient ($B_{2,\text{rep}} = 4$) is correct for the vdW equation and becomes worse with increasing f-value. The third virial coefficient ($B_{3,\text{rep}} = 10$) is correct for $f = (4 - 10^{0.5})/4 = 0.20943$.

It would be desirable to introduce a volume translation that leaves the second virial coefficient unchanged at the correct value, $B_{2,\text{rep}} = 4$. A simple way to correct the volume translation with respect to the second virial coefficient is to add the term $4fy$, which has been substracted before by the volume translation method

$$Z_{\text{rep}} = \frac{1}{1-(4-4f)y} + 4fy \tag{12}$$

Rearrangement and addition of the attraction term lead to a corresponding pressure equation

$$p = \frac{RT}{V+c-b} + c\frac{RT}{V^2} - \frac{a}{(V+c)^2} \tag{13}$$

It appears that improvement of the equation of state with respect to the virial coefficients increases the order of the equation from cubic to fifth order. Although this equation is not cubic anymore, we investigate its properties in order to analyze the effect of such correction. The repulsive virial coefficients calculated from Eq. 13 are the same as shown in Figure 1, with the exception of the second virial coefficient.

Figures 5 show the critical properties calculated with Eq. 13 as a function of f in the reduced units: $T^* = T \cdot Rb/4a$, $p^* = p \cdot b^2/16a$, $y = b/4V_m$, and $Z = p^*/T^*y$. These units can easily be related to real units by $T = T^* \cdot T_c/T_c^*$ and $p = p^* \cdot p_c/p_c^*$. One can see that for fixed $B_2 = 4$ the volume translation also affects the reduced critical pressure and temperature. The resulting compressibility factor is very similar to that calculated with the volume translation up to $f = 0.6$, which is close to the physical limit. Figures 6 show the phase equilibria calculated with Eq. 13 in comparison to the calculations with Eq. 3. It appears that for fixed $B_{2,\text{rep}} = 4$ one can obtain a similar coexistence curve, but at different f-values.

Temperature-Dependent Volume Translation

It is known that an empiric temperature-dependent volume translation can lead to a crossing of the isotherms (Pfohl, 1999). On the other hand, it is known that the perturbation theory for soft-sphere fluids yields an equation of state that consists of a hard-sphere reference term with a temperature-dependent covolume parameter (Barker and Henderson, 1967). Both kinds of temperature dependences enter the equation of state in a similar way. This raises the question whether a temperature-dependent volume translation always leads to unphysical behavior. In Figure 7 two possibilities for the effect of the temperature dependence on the isotherms are shown. We assume that each of these isotherms has a different pole-packing fraction originating from the temperature-dependent volume translation. If the isotherm at a lower temperature has a lower pole-packing fraction than the isotherm at a higher temperature, a crossing of these two isotherms cannot be avoided. It follows that crossing can be avoided if the pole-packing fraction decreases with increasing temperature

$$\left(\frac{\partial y_{\text{pole}}}{\partial T}\right) \le 0 \tag{14}$$

This can be regarded as a general condition. For the equation of state employed here, one can easily apply this condition

$$\left(\frac{\partial y_{\text{pole}}}{\partial f}\right)\left(\frac{\partial f}{\partial T}\right) \le 0 \tag{15}$$

With Eq. 10, it follows that

$$\frac{4}{(4-4f)^2}\left(\frac{\partial f}{\partial T}\right) \le 0 \tag{16}$$

Since the first term is always positive, it follows that, for noncrossing isotherms

$$\left(\frac{\partial f}{\partial T}\right) \leq 0 \tag{17}$$

For the simple case of a linearly temperature-dependent volume-translation parameter

$$f = AT + B \tag{18}$$

one obtains noncrossing isotherms for $A < 0$. For further analysis we calculate the packing fraction at the crossing of two isotherms and compare it to the pole-packing fraction for different values of A at constant B. The result is shown in Figure 8. In this calculation, $B = 0.5$ is used. Other values of B do not change the topology, they just change the range of the packing fraction. One can see that for $A < 0$ the pole-packing fraction, y_{pole}, is at lower values than the packing fraction at the isotherm crossing, y_{crossing}. Hence, the isotherm crossing is hidden behind the pole of the isotherm. For $A > 0$, the packing fraction at the isotherm crossing is at lower values than the pole of the equation of state. Therefore, the crossing of the isotherms can be observed.

Based on this investigation one can analyze empirical correlations given in the literature. Ungerer and Batut (1997), for example, suggested a linearly temperature-dependent volume translation in which the two parameters of the linear equation depend on the molecular weight. By setting $A = 0$, one can obtain the molecular weight at which an isotherm crossing can appear or vanish. Since in most cases nonlinear temperature dependences are employed, one can locate a possible isotherm crossing by calculating $\partial f/\partial T$.

While the analysis just given can help in the development of a consistent empirical equation of state, it is of interest to investigate theoretical approaches in a similar fashion. As mentioned earlier, it is known that a temperature-dependent covolume also can lead to a crossing of the isotherms (Salim and Trebble, 1991; Polishuk et al., 2000b). This can be easily understood if one compares, on a purely mathematical basis, the volume translation to the result of the perturbation theory for soft repulsion as given by Barker and Henderson (1967). This soft-sphere theory is based on a perturbed hard-sphere model and suggests a monotonically decreasing covolume with increasing temperature. This can be explained in a kinetic picture that suggests that soft spheres penetrate deeper with increasing temperature, which corresponds to the increasing velocity of the molecules, and, hence, the effective diameter decreases with increasing temperature. If one compares the vdW repulsion term with a temperature-dependent covolume, $RT/(V_m - b(T))$ to the expression of the volume translation, $RT/(V_m + c(T) - b)$, it follows that the slope of the temperature dependence of the soft sphere model has the opposite sign as for the volume-translation method. Hence, the analogous criterion corresponding to Eq. 17 for the temperature-dependent covolume parameter is

$$\left(\frac{\partial b}{\partial T}\right) > 0. \tag{19}$$

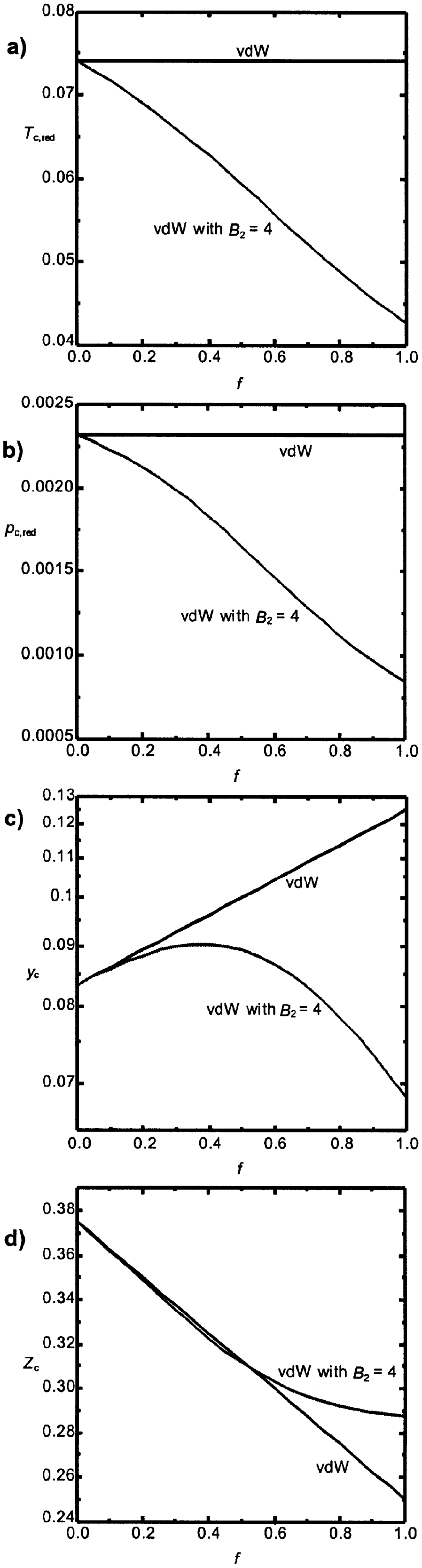

Figure 5. Critical properties as a function of the volume-translation parameter, *f*, calculated with Eq. 13 compared to the results obtained from Eq. 3.

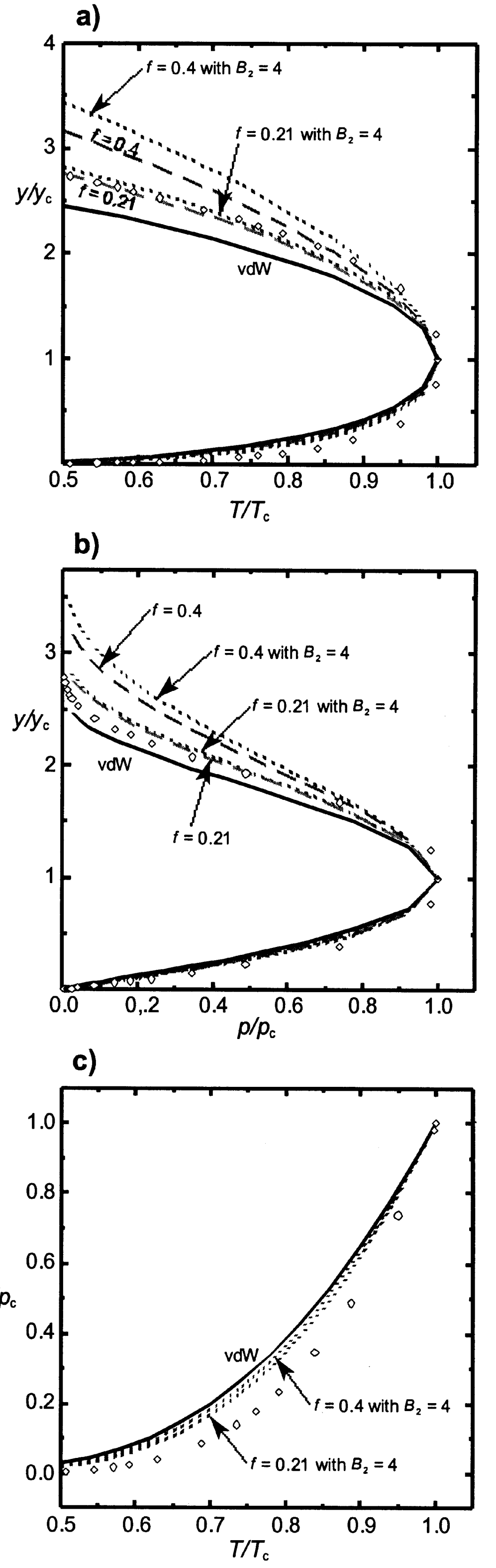

Figure 6. Comparison of the phase equilibria calculated with Eq. 3 and Eq. 13 for different values of the volume translation parameter, *f*.

All data are reduced by their critical values. The symbols are experimental data for the coexistence curve of methane (Vargaftik, 1975).

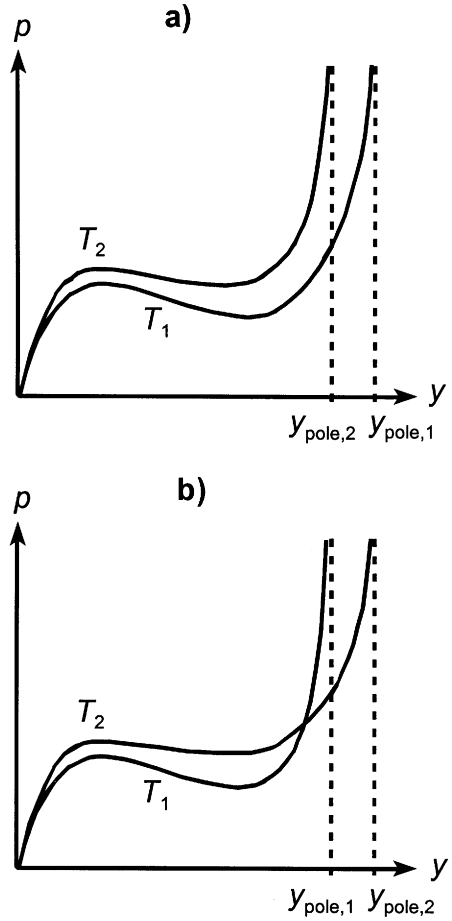

Figure 7. Two isotherms with different pole-packing fractions y_{pole}.

(a) No isotherm crossing appears if the pole-packing fraction decreases with increasing temperature. b) If the pole-packing fraction increases with increasing temperature, a crossing of the isotherms can appear.

This condition is not fulfilled in the perturbation theory for soft spheres, which is the reason for the crossing of the isotherms if applied to the van der Waals repulsion. However, it should be mentioned that the isotherm crossing often, but not necessarily, appears at high density. Perturbation theory is by definition only valid for small perturbations.

Furthermore, it has been mentioned in the literature (Ungerer and Batista de Sant'Ana 1999) that temperature-dependent volume translation can lead to negative values of the isobaric thermal expansion coefficients, α, at high pressure. If this is the case, then there must be an assumedly high-density or packing fraction at which the isobaric thermal expansion coefficient is zero or diverge to infinity. The effort of this section is to investigate this problem by locating this packing fraction. The isobaric thermal expansion coefficient is defined as

$$\alpha = \frac{1}{V}\left(\frac{\partial V}{\partial T}\right)_p \tag{20}$$

One can rewrite α as

$$\alpha = -\frac{1}{V}\frac{\left(\dfrac{\partial p}{\partial T}\right)_V}{\left(\dfrac{\partial p}{\partial V}\right)_T} \tag{21}$$

or in terms of the packing fraction

$$\alpha = \frac{1}{y}\frac{\left(\dfrac{\partial p}{\partial T}\right)_y}{\left(\dfrac{\partial p}{\partial y}\right)_T} \tag{22}$$

Based on Eq. 22 we can locate the packing fractions at which α becomes zero or diverges. This packing fraction is a boundary of the region with positive and negative α values. There are two possibilities for a change in the sign of α: first $(\partial p/\partial y)_T$ can change the sign, which happens at the spinodal. Since $(\partial p/\partial y)_T$ is in the nominator, the change of sign passes through a divergence. It follows that in the unstable region of the phase diagram, α is negative. This is the case for all equations of state independent of the volume translation. Secondly, $(\partial p/\partial T)_y$ can change the sign, which is the actual relevant condition for the analysis of a temperature-dependent volume translation. We have calculated the packing fraction for $(\partial p/\partial T)_y = 0$ at the same conditions as in the calculation of the isotherm crossing shown in Figure 8. It turns out that the packing fraction at which α crosses zero has the same numerical value as the packing fraction of the isotherm crossing with Eq. 18. An analysis of this result with a generic temperature dependence $f(T)$ is not feasible because it would require the solution of polynoms of the fifth order. However, it is comprehensible that the crossing of isotherms leads to a change in the sign of $(\partial p/\partial T)_y$ and α. It should also be mentioned that most equations of state have a temperature dependence in the attraction term, which can be used for the empirical optimization of the accuracy of an equation of state (see, for example, Polishuk et al., 2000a). Such temperature dependence may lead to additional complications, for example, if the temperature dependence of the attraction term passes through a minimum. As shown recently, in such cases it is advisable to decrease the numerical contribution of the temperature-dependent attraction term by modifying the repulsion term (Polishuk et al., 2002) in order to avoid further complications. In the context of the model investigated here, this would mean increasing the value of B in Eq. 18.

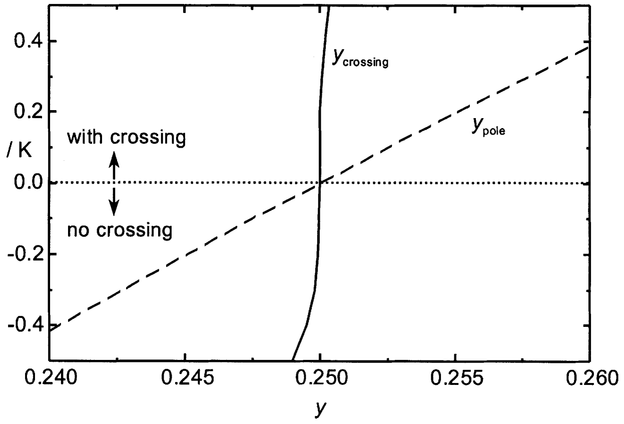

Figure 8. Comparison of the pole packing fraction with the packing fraction y_{pole} (dashed curve) and the packing fraction at the crossing of the isotherms y_{cross} (solid curve) for different values of A in Eq. 18.

The calculations are for $B = 0$, $T^* = 0.1$, $\Delta T^* = 0.002$. The crossing point is calculated by $p^*(T^*) = p^*(T^* + \Delta T^*)$, with $p^* = ZyT^*$ and Z as given by Eq. 4.

Nonclosed-Form Equation of State Approaches

Another problem that has been discussed in the literature is the possibility of negative heat capacities when a temperature-dependent covolume is employed. It appears that the modeling of soft-sphere fluids at high pressure and density based on a closed-form perturbed hard-sphere approach has a general shortcoming. While $(\partial b/\partial T) < 0$ leads to isotherm crossing, a positive curvature $(\partial^2 b/\partial T^2)$ can lead to negative c_p at high pressure, as suggested by Trebble and Bishnoi (1986). In order to investigate this problem we here employ the theoretically based virial equation of state. First we choose a simple soft-repulsive fluid without attraction in order to investigate the soft repulsion separately. The virial equation is truncated after the second term

$$p = \frac{RT}{V}\left(1 + \frac{B(T)}{V}\right) \tag{23}$$

Due to the truncation this equation is physically valid at low densities or high molar volumes. However, it is used here for the investigation of the mathematical structure of an equation of state, and in this context, it is also used at higher densities. As we will show later, this is reasonable because the higher repulsive virial coefficients behave topologically similar to the repulsive second virial coefficient, for example, they decrease monotonically with increasing temperature. It follows that accounting for higher repulsive virial coefficients changes Eq. 23 quantitatively, but not qualitatively.

The second virial coefficient can be calculated from the soft-repulsion potential by Eq. 24 (McQuarrie, 1976). We use the reduced variables: $B^* = B/\sigma^3$, $r^* = r/\sigma$, and $T^* = T/\tilde{T}$, where $\tilde{T}$ is the characteristic temperature defined as $\tilde{T} = \epsilon/k_B$, with the depth of the pair potential ϵ, and the Boltzmann constant k_B

$$B^*(T^*) = -2\pi\int_0^\infty \left(\exp\left(-\frac{u^*(r^*)}{T^*}\right) - 1\right)(r^*)^2 dr \tag{24}$$

Here the soft repulsive r^{-12}-potential is used

$$u^*(r^*) = 4\left(\frac{1}{r^*}\right)^{12} \tag{25}$$

The evaluation of Eq. 24 gives the following equation for the reduced second virial coefficient of the repulsive r^{-12}-potential as function of the reduced temperature

$$B^*(T^*) = 3.6295886 \cdot (T^*)^{-1/4} \tag{26}$$

If we insert the second virial coefficient into the virial equation (Eq. 23), we obtain with $q \equiv \sigma^3 N_L$

$$p = \frac{RT}{V_m}\left(1 + \frac{B^*(T/\tilde{T}) \cdot q}{V_m}\right) \tag{27}$$

The isochoric heat capacity for a general temperature dependence of the second virial coefficient is given by Eq. 28

$$\frac{c_V - c_V^*}{R} = -\frac{q}{V}(T^*)^2\left\{2\left(\frac{\partial B^*}{\partial T}\right) + T^*\left(\frac{\partial^2 B^*}{\partial T^2}\right)\right\} \tag{28}$$

Here c_V^* is the ideal gas contribution to the isochoric heat capacity. It shows that a combination of the first and second temperature derivatives determines the sign of $(c_V - c_V^*)/R$. For the isobaric heat capacity one similarly gets a combination of the first and second temperature derivatives; however, the expression is lengthy and omitted here. One can now calculate the isochoric heat capacity by inserting Eq. 26 into Eq. 28, which can be rearranged to

$$\frac{c_V - c_V^*}{R} = \frac{3}{16}\,\frac{q \cdot B^*(T^*)}{V_m} \tag{29}$$

Since $(c_V - c_V^*)/R$ behaves as $B^*(T^*)$, it exhibits no negative values. For the isobaric heat capacity, we obtain

$$\frac{c_p - c_p^*}{R} = \frac{27 V_m q B^*(T^*) + 15\left[qB^*(T^*)^2\right] + 16 V_m^2}{16 V_m\left[V_m + 2qB^*(T^*)\right]} \tag{30}$$

Since the second repulsive virial coefficient is always positive, it follows that the isobaric heat capacity is also always positive. Furthermore, as mentioned earlier, the criterion for isotherm crossing is the vanishing of the derivative of the pressure with respect to the temperature. With Eq. 27 one obtains

$$\left(\frac{\partial p}{\partial T}\right)_V = \frac{R\left[V_m + 3/4 \cdot q \cdot B^*(T^*)\right]}{V_m^2} = 0 \tag{31}$$

The solution is $V_m = -3/4 \cdot q \cdot B^*(T^*)$, which is always negative, and, hence, not in the physically relevant range. Another solution can be found in the ideal gas limit $\lim_{V_m \to \infty} (\partial p/\partial T)_V = 0$, which all together indicates that there is no isotherm crossing for Eq. 27 if used with Eq. 26. Since at the same time the isochoric and the isobaric heat capacities are always positive, such an approach for a soft repulsive fluid appears to be consistent in the context of the properties investigated here.

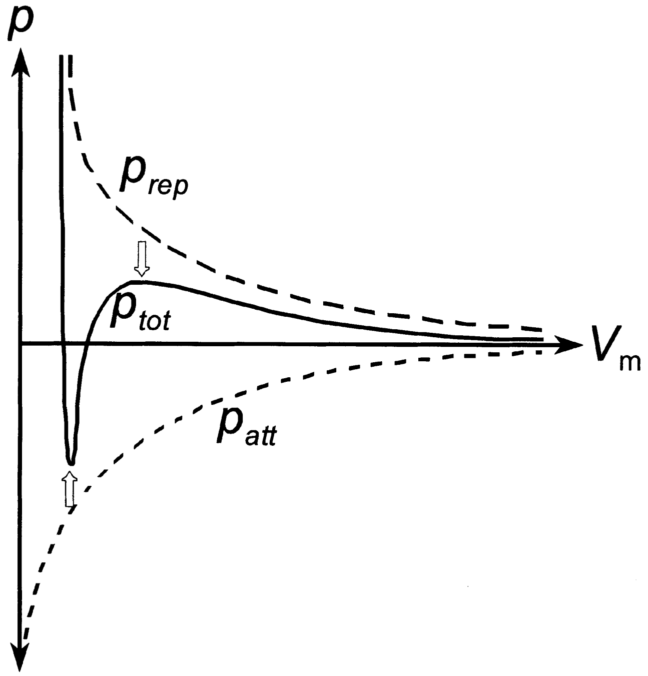

Figure 9. Attractive and repulsive contribution of a subcritical isotherm in the pressure-volume diagram.

While both contributions are monotonous functions, the sum of both exhibits two extremes at which the derivative of the pressure with respect to the volume vanish. They are marked with arrows.

Since Eq. 27 is only valid for low densities, we added the third virial coefficient, C, into the equation of state in order to investigate the influence of higher repulsive virial coefficients. The virial equation is then given by

$$p = \frac{RT}{V}\left(1 + \frac{B(T)}{V} + \frac{C(T)}{V^2}\right) \tag{32}$$

Introducing the reduced third virial coefficient, C^*, defined by $C(T) = \sigma^6 C^*(T/\tilde{T})$, we obtain

$$p = \frac{RT}{V_m}\left(1 + \frac{B^*(T/\tilde{T}) \cdot q}{V_m} + \frac{C^*(T/\tilde{T}) \cdot q^2}{V_m^2}\right) \tag{33}$$

Evaluation of the equation for the repulsive third virial coefficient (McQuarrie, 1976), analogous to Eq. 24 for the second virial coefficient, gives the following result

$$C^*(T^*) = 7.5821325 \cdot (T^*)^{-1/2} \tag{34}$$

The investigation of Eq. 33 gives basically the same results as discussed previously for Eq. 27, that is, positive isochoric and isobaric heat capacities and positive isobaric thermal expansion coefficient. The results are included in Figure 10a and 10c, which will be discussed in detail later. This behavior can be explained by the fact that the third soft repulsive virial

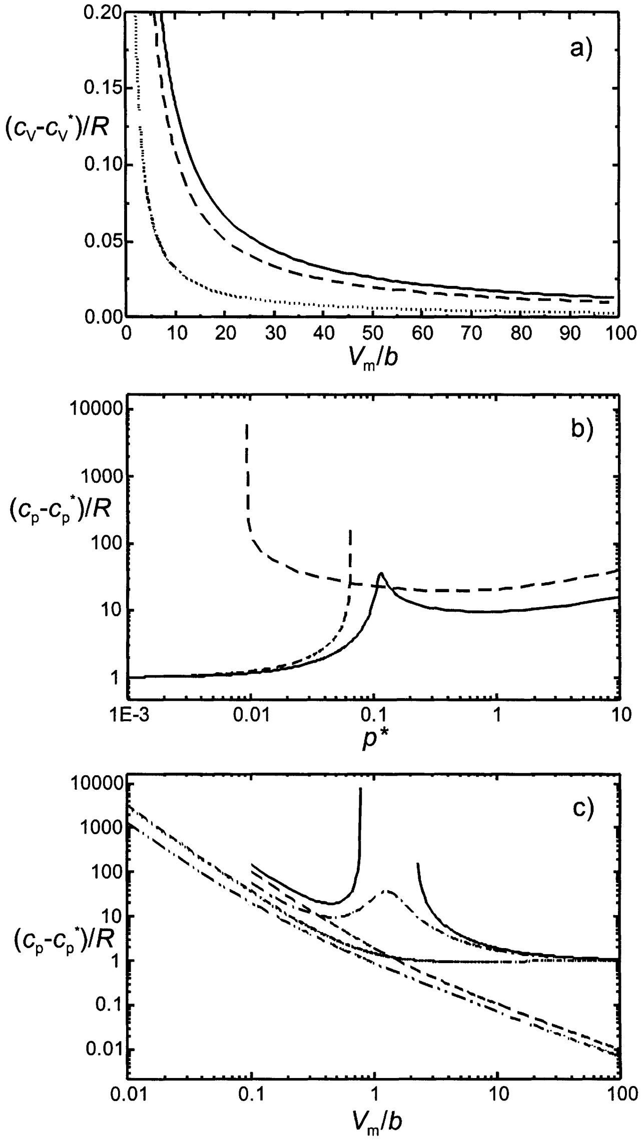

Figure 10. Residual isochoric and isobaric heat capacity.

(a) Residual isochoric heat capacity as function of the reduced volume at the reduced temperature $T^* = 1.333$. Dashed curve: attractive contribution; dotted curve: repulsive contribution; solid curve: complete potential. (b) Residual isobaric heat capacity as function of the reduced pressure $p^* = pb/4R\tilde{T}$ for different reduced temperatures: dashed curve: $T^* = 1.333$; solid curve: $T^* = 1.5$. (c) Residual isobaric heat capacity as function of the reduced volume for different reduced temperatures. Solid: complete potential at $T^* = 1.333$; dot-dashed: complete potential at $T^* = 1.5$; dashed: attractive potential at $T^* = 1.333$; dot-dot-dashed: attractive potential at $T^* = 1.5$; dotted and dash-dash-dotted: repulsive potential at $T^* = 1.333$ and at $T^* = 1.5$ (nondistinguishable in this scale).

coefficient is as monotonically decreasing as the second one. Since such behavior can also be expected for the higher virial coefficients, one can conclude that the results of the investigation of Eq. 27 can also be extrapolated to the virial equations of state with a higher virial coefficients, and, hence, valid at higher densities.

However, results of the investigation of the repulsive contribution to the isobaric heat capacity cannot represent the behavior of the total molecular potential, which includes a repulsive and an attractive part. One can obtain the equation for c_p by Jacobi transformation of the derivatives of the enthalpy and the pressure with respect to the temperature and volume as given by Eq. 35

$$c_p = \left(\frac{\partial H}{\partial T}\right)_V - \left(\frac{\partial H}{\partial V}\right)_T \frac{\left(\frac{\partial p}{\partial T}\right)_V}{\left(\frac{\partial p}{\partial V}\right)_T} \tag{35}$$

This equation reveals that the total isobaric heat capacity cannot be separated into a sum of the attractive and the repulsive parts. The crucial property is the second term, which makes it nonadditive, such as, for example, $(\partial p/\partial V)$ in the denominator of Eq. 35. As shown in Figure 9 the repulsive and attractive contributions to the pressure are monotonic functions of the volume. However, the total pressure, which is the sum of both, exhibits for a subcritical isotherm two extremes at the spinodal. At these extremes $(\partial p/\partial V)$ is zero, and, hence, c_p diverges. This is a similar divergence as observed at the critical point. Since c_p, calculated for the attractive and the repulsive terms separately, do not exhibit these divergences, one cannot separate c_p into the attractive and repulsive contributions. This shows that approaches for locating negative c_p for a certain equation of state that are only based on a repulsion term, such as the van der Waals repulsion, are not meaningful.

Up to now, we have only investigated the repulsive soft-sphere fluid. However, this model is not representative for the isobaric heat capacity, as mentioned earlier. Now we use a similar approach that includes the second and the third virial coefficients, both of which are obtained from the complete Lennard-Jones potential including the attraction term. This equation of state can be used to calculate vapor–liquid phase equilibria, since it includes the attractive and repulsive parts of the second and third virial coeffcients. Figure 10 shows the heat capacities calculated from Eq. 32 using the Lennard-Jones virial coefficients given by Hirschfelder et al. (1954). The heat capacities behave well, that is, they are positive. This model does also not exhibit isotherm crossing. Hence, Eq. 32 is consistent with respect to the properties investigated here. In Figure 10a the isochoric heat capacity is plotted for the attractive and the repulsive contributions and for the complete potential. It appears that all contributions are positive. The isobaric heat capacity is plotted in Figure 10b as a function of the pressure. Here, only c_p is plotted for the total potential, because the attractive contribution is at negative pressure. One can recognize the divergence at the spinodal for the subcritical isotherm. It remains as a sharp maximum for the supercritical isotherm. In order to compare the different contributions, in Figure 10c we plotted the isobaric heat capacity as a function of the volume. One can see that repulsive and attractive contributions are monotonous functions and the sum of both can neither cause a maximum nor a divergence, as discussed earlier. In all cases investigated in this section, the isobaric and the isochoric heat capacities are positive and tend to increase with increasing pressure or decreasing molar volume. Therefore, this model for the soft-sphere fluid does not exhibit negative heat capacities at high pressure.

This investigation shows that the approach for describing the soft-sphere fluid by a perturbed hard-sphere model is the source of the inconsistencies at high pressure. Specifically, it is the closed form of such equations with a $1/(V_m - b)$ or a $1/(1 - y)$ term for the hard-sphere reference equation that is responsible for that behavior. The reason for these inconsistencies is the fact that the equations for the hard-sphere reference fluid have a pole at a certain packing fraction. This pole is related to the limiting behavior of the higher virial coefficients (Yelash and Kraska, 2001) and reflects the hardness of the molecules. Soft spheres are penetrable, and, hence, there is no distinct highest packing fraction and no pole in the equation of state.

As shown earlier it is not justifiable to analyze the isobaric heat capacity based on only one term of an equation of state. For equations of state without a temperature-dependent covolume, the residual repulsion term (repulsion minus the ideal gas contribution) vanishes due to the differentiation and makes no contribution to the heat capacities. Therefore, the residual heat capacities are in such cases modeled by the attraction term only. However, at high pressure and density, where the isotherm crossing can appear, the repulsive forces are dominant for the fluid-phase behavior.

Conclusions

We have analyzed how the volume translation in an equation of state affects the virial coefficients, the critical properties, and several thermodynamic properties. While the temperature-independent volume translation improves the values of the higher virial coefficients, it worsens the value of the lower virial coefficient. Correcting the volume-translation technique with respect to the accurate value of the second virial coefficients of the repulsion term affects the mathematical structure of the equation of state. In general, introduction of physical constraints, such as fixing the second virial coefficient to its theoretical value, leads to an increase in the mathematical order of the equation. One can conclude that a temperature-independent volume translation is a possibility to maintain the original equation-of-state structure at the cost of the accuracy of the lower virial coefficients. An alternative may be a mapping approach, which is based on a detailed analysis of the virial coefficients (Yelash, 2002; Yelash and Kraska, 1999b; Yelash et al., 1999a,b; Yelash and Kraska, 2001) and has been applied for deriving simplified equations of state.

Furthermore, we have investigated how a temperature-dependent volume translation affects the equation-of-state properties. It turns out that a volume-translation parameter that decreases with temperature does not lead to an isotherm crossing. For a temperature-dependent covolume, the situation is the opposite. The shortcomings of the models that exhibit negative heat capacities and isotherm crossing could be traced back to the mathematical structure of the closed-form perturbed hard-sphere approaches. However, since perturbation theories are per definition valid only for small perturbations, the inconsistencies at high density and pressure are the result of using a perturbation theory beyond its valid range. It follows that in such cases even physically based approaches can lead to unphysical behavior. On the other hand, as shown in the first part of this investigation, empirical approaches are not necessarily wrong just because of their empirical character. Approaches of both kinds have to undergo a topological analysis as, for example, suggested here.

Acknowledgments

The authors thank the Deutsche Forschungsgemeinschaft and the Fonds der Chemischen Industrie for supporting this work.

Literature Cited

Ahlers, J., and J. Gmehling, "Development of an Universal Group Contribution Equation of State I. Prediction of Liquid Densities for Pure Compounds with a Volume Translated Peng-Robinson Equation of State," *Fluid Phase Equilib.,* **191**, 177 (2001).

Barker, J. A., and D. Henderson, "Perturbation Theory and Equation of State for Fluids. II. A Successful Theory of Liquids," *J. Chem. Phys.,* **47**, 4714 (1967).

Chou, G. F., and J. M. Prausnitz, "A Phenomenological Correction to an Equation of State for the Critical Region," *AIChE J.*, **35**, 1487 (1989).

Carnahan, N. F., and K. E. Starling, "Equation of State for Nonattracting Rigid Spheres," *J. Chem. Phys.*, **51**, 635 (1969).

Hirschfelder, J. O., C. F. Curtiss, and R. B. Bird, *Molecular Theory of Gases and Liquids*, Wiley, New York (1954).

Janse van Rensburg, E. J., "Virial Coefficients for Hard Discs and Hard Spheres," *J. Phys. A,* **26**, 4805 (1993).

Jhaveri, B. S., and G. K. Youngren, "Three Parameter Modification of the Peng-Robinson Equation of State to Improve Volumetric Prediction," *SPE Reservoir Eng.*, **8**, 1033 (1988).

Ji, W.-R., and D. A. Lempe, "Density Improvement of the SRK Equation of State," *Fluid Phase Equilib.*, **130**, 49 (1997).

Martin, J. J., "Cubic Equations of State—Which?," *Ind. Eng. Chem. Fundam.*, **18**, 81 (1979).

McQuarrie, D. A., *Statistical Mechanics*, Harper Collins, New York (1976).

Peneloux, A., E. Rauzy, and R. Fréze, "A Consistent Correction for Redlich-Kwong Volumes," *Fluid Phase Equilib.*, **8**, 7 (1982).

Peng D. Y., and D. B. Robinson, "A New Two-Constant Equation of State," *Ind. Eng. Chem. Fundam.*, **15**, 59 (1976).

Pfohl, O., "Evaluation of an Improved Volume Translation for the Prediction of Hydrocarbon Volumetric Properties," *Fluid Phase Equilib.,* **163,** 157 (1999).

Polishuk, I., J. Wisniak, and H. Segura, "A Novel Approach for Defining Parameters in a Four-Parameter EOS," *Chem. Eng. Sci.,* **55**, 5705 (2000a).

Polishuk, I., J. Wisniak, H. Segura, L. V. Yelash, and T. Kraska, "Prediction of the Critical Locus on Binary Mixtures Using Equation of State: II. Investigation of van der Waals-Type and Carnahan-Starling-Type Equations of State," *Fluid Phase Equilib.*, **172,** 1 (2000b).

Polishuk, I., J. Wisniak, H. Segura, and T. Kraska, "About the Relation Between the Empirical and Theoretically Based Parts of van der Waals-Like Equations of State," *Ind. Chem. Eng. Res.*, **41**, 4414 (2002).

Redlich, O., and J. N. S. Kwong, "On the Thermodynamics of Solutions. V: An Equation of State. Fugacities of Gaseous Solutions," *Chem. Rev.*, **44**, 233 (1949).

Ree, F. H., and W. G. Hoover, "Fifth and Sixth Virial Coefficients for Hard Spheres and Hard Disks," *J. Chem. Phys.*, **40**, 939 (1964).

Ree, F. H., and W. G. Hoover, "Seventh Virial Coefficients for Hard Spheres and Hard Disks," *J. Chem. Phys.*, **46**, 4181 (1967).

Salim, P. H., and M. A. Trebble, "A Modified Trebble-Bishnoi Equation of State: Thermodynamic Consistency Revisited," *Fluid Phase Equilib.,* **65**, 59 (1991).

Trebble, M. A., and P. R. Bishnoi, "Accuracy and Consistency of Ten Cubic Equations of State for Polar and Non-Polar Compounds," *Fluid Phase Equilib.*, **29**, 465 (1986).

Ungerer, P., and H. Batista de Sant'Ana, "Reply to the Letter to the Editor by O. Pfohl About the Paper 'Evaluation of an Improved

Volume Translation for the Prediction of Hydrocarbon Volumetric Properties'," *Fluid Phase Equilib.,* **163,** 161 (1999).

Ungerer, P., and C. Batut, "Prediction des Proprietes Volumetriques des Hydrocarbures par une Translation de Volume Amelioree," *Rev. de 'Inst. Fr. Pét.*, **52**, 609 (1997).

Vargaftik, N. B., *Tables on the Thermophysical Properties of Liquids and Gases*, Wiley, New York (1975).

Yelash, L. V., and T. Kraska, "Investigation of a Generalized Attraction Term of an Equation of State and Its Influence on the Phase Behaviour," *Fluid Phase Equilib.*, **162,** 115 (1999a).

Yelash, L. V., and T. Kraska, "Statistical Associating Fluid Theory for Chains of Attractive Hard-Spheres: Optimized Equation of State," *Phys. Chem. Chem. Phys.,* **1**, 2449 (1999b).

Yelash, L. V., T. Kraska, A. E. Müller, and N. F. Carnahan, "Simplified Equation of State for Non-Spherical Hard Particles: An Optimized Shape Factor Approach," *Phys. Chem. Chem. Phys.*, **1**, 4919 (1999a).

Yelash, L. V., T. Kraska, and U. K. Deiters, "Closed-Loop Critical Curves in Simple Hard-Sphere van der Waals-Fluid Models Consistent with the Packing Fraction Limit," *J. Chem. Phys.*, **110,** 3079 (1999b).

Yelash, L. V., and T. Kraska, "A Generic Equation of State for the Hard-Sphere Fluid Incorporating the High Density Limit," *Phys. Chem. Chem., Phys.*, **3**, 3114 (2001).

Yelash, L. V., "Development of Equations of State for Complex Fluids," PhD Thesis, VDI-Verlag, Düsseldorf (2002).

Manuscript received June 7, 2002, and revision received Nov. 13, 2002.